Prosimy cytować jako: Inż. Ap. Chem. 2013, 52, 6, 541-542

Marcin LEMANOWICZ, Grzegorz DZIDO, Andrzej GIERCZYCKI, Mateusz WITKOWSKI, Michał DRZAZGA

e-mail: marcin.lemanowicz@polsl.pl

Department of Chemical Engineering and Process Design, Faculty of Chemistry, Silesian University of Technology, Gliwice, Poland

Numerical simulation of nanofluid flow in a small diameter pipe

Introduction

The nanofluids are of great interest to the scientific world as well to the industry. These fluids exhibit some interesting properties like enhancement of heat transfer or catalysis of different chemical reactions [*Burton et al., 2011; Khedkar et al., 2012*]. By definition nanofluid is a multiphase system of nanometer size particles suspended in a carrier fluid [*Drzazga et al., 2012*]. The dispersed phase consist of metal, metal oxide, nanotubes etc. whereas the continuous phase is water, ethylene glycol and others. At present, an interested reader may find many publications concerning simulation of nanofluids flow using Computational Fluid Dynamics (CFD) [*Moraveji and Esmaeili, 2012*]. The usual considerations involve comprehensive comparison of the heat transfer coefficient taking into account different geometries, nanofluid concentrations, particle sizes and types. On the other hand, it is hard to find any papers dedicated to simulations of the pressure drop during nanofluid flow. In authors opinion this issue should not be omitted since the pump power may limit the application of nanofluid in some cases like cooling of electronic equipment [*Selvakumar and Suresh, 2012*] since the nanofluid would be transferred though the small diameter channels.

The goal of this work was to perform a CFD analysis of the pressure drop during nanofluid flow through a small diameter pipe. The numerical results were compared with experimental data.

Experimental

The detailed description of materials, laboratory setup and the measurement procedure are presented in the another paper [*Drzazga et al., 2013*]. In this paper the results concerning nanofluids without addition of surfactants are presented. In this research copper(II) oxide water-based nanofluid was used. Nanoparticles of 30÷50 nm diameter were obtained from *Nanostructured & Amorphous Materials Inc.* (USA). The nanofluid was produced in a two step procedure. In the first step a proper amount of nanopowder was weighted and suspended in reverse osmosis water (*Hydrolab*, Poland). Moreover, triammonium citrate was added in order to stabilize the nanosuspension. Then, the mixture was continuously circulated through the ultrasonic mixer (*VCX-730 by Sonics*, USA) to break up agglomerates. A volume concentration of nanoparticles was 1%. The laboratory stand consisted of a fluid tank, centrifugal pump and a smooth copper pipe of 12 mm diameter which was mounted into two brass heads. The pressure drop was measured by a differential pressure transducer NPXD 2 (Peltron, Poland) on the distance of 945 mm. Flow rate in the setup was measured by magnetic flowmeter *Flowmex PV 40* (*Codea*, Czech Republic).

Numerical simulations

The simulations of nanofluid flow using computational fluid dynamics may be realized using two different methodologies, i.e. one phase simulation or multiphase simulation [*Moraveji and Esmaeili, 2012*]. In the first case, the considerations are limited to just one phase which has to be represented by a system of functional dependences between the physical properties of the nanofluid and the intrinsic characteristics of introduced nanoparticles as well as their volume fraction in the mixture. In the second case, both carrier fluid as well as the nanoparticles are considered as separate phases. Such approach yields in more detailed information about the movement of the dispersed phase, its homogeneity as well as its impact on the flow. Consequently, it requires more resources regarding computational and memory capabilities. In the presented research both methodologies were used in order to perform the CFD simulations. The geometrical model and numerical mesh (Fig. 1) were created using *ANSYS Workbench 14.5* environment. In order to eliminate the impact of mesh refinement on the final results the grid-independence study was performed. The results of assessment for the optimal mesh and meshes with +/-10% of elements are presented in Tab. 1.

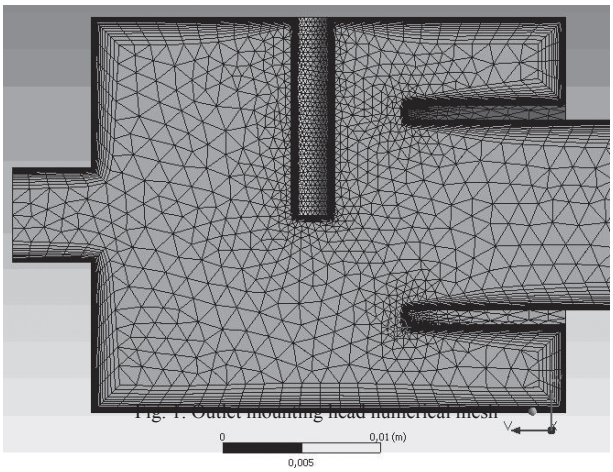

Fig. 1. Outlet mounting head numerical mesh

Tab. 1. Numerical mesh quality

Number of nodes		383 871	433 022	468 070
Number of elements		844 371	959 407	1 040 021
Skewness	Average	0.23	0.22	0.20
	Standard deviation	0.15	0.15	0.14
Orthogonal quality	Average	0.88	0.89	0.90
	Standard deviation	0.16	0.15	0.15
Deviation of pressure drop [%]		0.40	–	1.38

The optimal mesh represented the laboratory stand divided by a vertical symmetry plane (half of the model) and it consisted of tetrahedron elements (the smallest elements had size of 15e-05 m). Moreover a viscous layer consisting of 20 prism sub-layers was created in order to preserve Y^+ parameter below 5 (min. layer thickness 7e-07 m).

In both methodologies, i.e. single phase and multiphase, the standard k-ε turbulence model was employed [*Launder and Spalding, 1972*]:

$$\frac{\partial}{\partial t}(\rho k) + \frac{\partial}{\partial x_i}(\rho k u_i) = \frac{\partial}{\partial x_j}\left[\left(\mu + \frac{\mu_t}{\sigma_k}\right)\frac{\partial k}{\partial x_j}\right] + G_k + G_b - \rho\varepsilon + Y_M + S_k \quad (1)$$

$$\frac{\partial}{\partial t}(\rho \varepsilon) + \frac{\partial}{\partial x_i}(\rho \varepsilon u_i) = \frac{\partial}{\partial x_i}\left[\left(\mu + \frac{\mu_t}{\sigma_\varepsilon}\right)\frac{\partial \varepsilon}{\partial x_j}\right] + C_{1\varepsilon}\frac{\varepsilon}{k}(G_k + C_{3\varepsilon}G_b) - C_{2\varepsilon}\rho\frac{\varepsilon^2}{k} + S_\varepsilon \quad (2)$$

with model constants: $C_{1\varepsilon} = 1.44$, $C_{2\varepsilon} = 1.92$, $C_\mu = 0.09$, $\sigma_k = 1.0$, $\sigma_\varepsilon = 1.3$. Furthermore, the enhanced wall treatment was used in order to properly simulate turbulence in the near-wall region. All calculations were done using Fluent pressure based solver at the steady state. In all cases the inlet boundary condition was *velocity inlet* at the inlet brass head and *pressure outlet* at the outlet brass head. All walls had no slip condition with exception of the symmetry plane which obviously had the symmetry condition. The pressure-velocity coupling was done using SIMPLE scheme and the pressure discretization was achieved by the standard procedure. All interpolation schemes were of second order upwind. In case of multiphase simulations mixture model was used. The

Prosimy cytować jako: Inż. Ap. Chem. 2013, 52, 6, 541-542

second phase (solid particles of 40 nm diameter) volumetric fraction was calculated using first order upwind scheme. All simulations were run until scaled residuals achieved convergence at 10^{-5} value.

Results

Fig. 2 presents plots of the experimental, numerical and theoretical pressure drop values for five velocities which represents *Reynolds* number range from 5 000 to 15 000. As it can be seen the CFD data correspond quite closely to the theoretical values obtained directly from the *Blasius* equation:

$$\lambda = \frac{0.3164}{Re^{0.25}} \quad (3)$$

which is valid for $Re = 3000 \div 100000$.

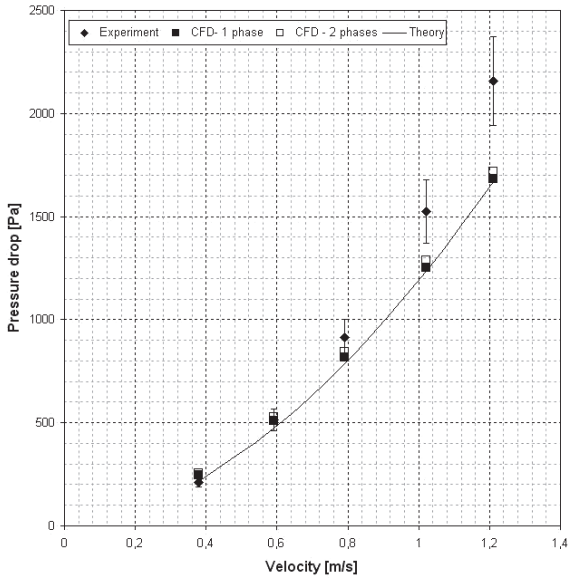

Fig. 2. Comparison between experimental results and CFD simulations

Experimental values, on the other hand, deviate from the simulation results by 25% for the highest investigated velocity. However high fluctuations of pressure drop readings resulting in 10% measurement error may be the explanation for such high differences between these results. It should be noticed that the data from both methodologies, i.e. single-phase and multiphase simulations, are very similar to each other and lie close to the analytical solution. What is interesting, the multiphase approach always resulted in slightly higher pressure drop values than single-phase approach. Moreover, during the analysis of the overall results it was proved that the multiphase approach predicted higher local pressure losses than in case of single-phase approach. These results are consistent with the pump power demand readings during the experiments, however this issue needs to be investigated in further research.

Fig. 3 pictures data for the outlet region of analyzed geometry for five different velocities, respectively. What can be observed it is that for the highest velocities the flow exhibits quite high level of uniformity in concentration. On the other hand, simulations for the lowest velocities showed certain fluctuation in concentration of the second phase. Referring to theoretical approaches considering nanofluids, nanosize of suspended particles makes them very similar to the uniform one-phase solutions, therefore balanced distribution of nanoparticles originating for the numerical analysis confirms such assumption of their general treatment. Some differences in concentration for lower velocities appears only in ”dead zones” of the outlet mounting head. The concentration of nanoparticles in the main flux was uniform. The above mentioned findings confirm conclusion of other authors [*Jafari et al., 2009; Moraveji and Esmaeili, 2012*] that the employment of single-phase methodology is justified only in case when the complex properties of nanofluid cannot be simulate using multiphase model or when the simulated phenomenon is relatively simple and there is need to limit the computational costs of calculations.

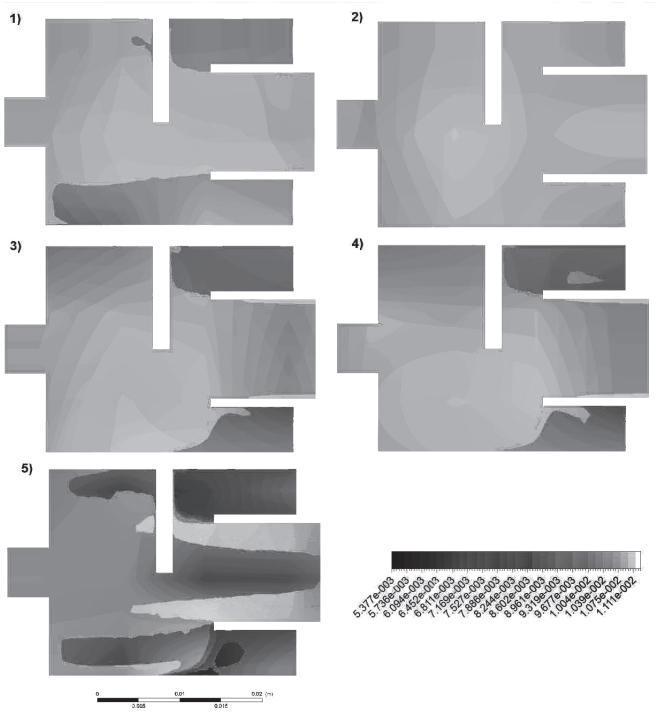

Fig. 3. Concentration of nanoparticles at outlet mounting head for five different velocities: 1) 1.21 m/s, 2) 1.02 m/s, 3) 0.79 m/s, 4) 0.59, 5) 0.38 m/s

Conclusions

The research concerning CFD simulation of CuO – water nanofluid pressure drop during flow through the 12 mm pipe was presented.

It was proved that either one-phase simulation as well as multiphase simulations resulted in good agreement with theoretical calculations and experimental results.

Nonetheless authors recommend to use the multiphase model if there is such possibility, although it is occupied by higher computational cost. The multiphase approach allows one to investigate the behavior of nanoparticles within the fluid and in some cases to reflect more complex phenomena that would not be predicted by the single-phase model.

LITERATURE

Burton P.D., Boyle T.J., Datye A.K., 2011. Facile, surfactant-free synthesis of Pd nanoparticles for heterogenous catalysts. *J. Catal.*, **280**, 2, 145-149. DOI: 10.1016/j.jcat.2011.03.022

Drzazga M., Lemanowicz M., Dzido G., Gierczycki A., 2012. Preparation of metal oxide-water nanofluids by two-step method. *Inż. Ap. Chem.*, **51**, nr 5, 213-215

Drzazga M., Gierczycki A., Dzido G., Lemanowicz M., 2013. Influence of non-ionic surfactant addition on drag reduction of water based nanofluid in a small diameter pipe. *Chin. J. Chem. Eng.*, **21**, 1, 104-108. DOI:10.1016/S1004-9541(13)60447-4

Jafari A., Mousavi S.M., Tynjala T., Sarkomaa P., 2009. *CFD simulation of gravitational sedimentation and clustering effects on heat transfer of a nano-ferrofluid* [in:] PIERS Proceedings. Beijing, China, 23-27 March 2009, 1352-1356

Khedkar R.S., Sonawane S.S. Wasewar K.L, 2012. Influence of CuO nanoparticles in enhancing thermal conductivity of water and monoethylene glycol based nanofluids. *Int. Commun. Heat Mass*, **39**, 5, 665-669. DOI:10.1016/j.icheatmasstransfer.2012.03.012

Launder D.B., Spalding B.E.., 1972. *Lectures in mathematical models of turbulence*. Academic Press, London, England.

Moraveji M.K., Esmaeili E., 2012. Comparison between single-phase and two-phases CFD modeling of laminar forced convection flow of nanofluids in a circular tube under constant flux. *Int. Commun. Heat Mass*, **39**, 8, 1297-1302. DOI: 10.1016/j.icheatmasstransfer.2012.07.012

Selvakumar P., Suresh S., 2012. Convective performance of CuO/water nanofluid in an electronic heat sink. *Exp. Therm. Fluid Sci.*, **40**, 57-63. DOI: 10.1016/j.expthermflusci.2012.01.033

This research was supported by the State Committee for Scientific Research (Poland) under grant no. NN209764040.